Fretting-Wear Characteristics of Steam Generator Tubes Contacting with Foreign Object

Jong Chull Jo, Myung Jo Jhung, Woong Sik Kim, and Hho Jung Kim

Korea Institute of Nuclear Safety
19 Guseong-dong, Yuseong-gu
Daejeon 305-338 Korea

Abstract

Fretting-wear characteristics of steam generator tubes contacting with foreign object has been investigated in this study. The operating steam generator shell-side flow field conditions are obtained from three-dimensional steam generator flow calculation using a well-validated steam generator thermal-hydraulic analysis computer code. Modal analyses are performed for the finite element modelings of tubes to get the natural frequency, corresponding mode shape and participation factor. The wear rate of a steam generator tube caused by foreign object is calculated using the Archard formula and the remaining life of the tube is predicted. In addition, the effects of internal pressure and flow velocity on the remaining life of the tube are discussed in this paper.

1. Introduction

During the outage of the nuclear power plant, a foreign object search and retrieval is performed in the secondary side of the steam generator (SG). During this operation, several objects may be found. Most of them are retrieved but some may be in such a position that removal would require additional tooling and this tooling is not available on site. If the object remains, the tube wear could develop since relative motion between the object and tubes would be possible. For the structural integrity of the U-tube in contact with this object to be assured during the next operating cycle, it is necessary to determine the effect of this object remaining in the secondary side of the SG.

Tube vibration excited by dynamic forces of external fluid flow in nuclear steam generators may either initiate such mechanical damages on tubes as fretting-wear and fatigue which may eventually result in severe tube failures or accelerate the wear of the tube by foreign object. Even less significant dynamic forces of external fluid flow exerting to tube which can not cause any damage to the tube may lead to excessive vibration resulting in failure of the tube due to fretting-wear. Therefore, with regard to nuclear safety, it is very important to assess the potential for SG tube failures due to fretting-wear to take the necessary preventive measures for minimizing the probability of SG tube failures in operating plants. The assessment of the potential for such a SG tube failure can be accomplished by performing the fretting-wear analysis by foreign object, for which the prerequisite is the performance of three-dimensional SG flow field calculation and tube modal analysis.

This study investigates the fretting-wear characteristics of steam generator U-tubes. The operating SG shell-side flow field conditions for determining the fretting-wear parameters such as flow velocity and added mass are obtained from three-dimensional SG flow calculation using the ATHOS3 code. Modal analyses are performed for the finite element modelings of U-tubes with various conditions. The effects of internal pressure on the modal and fretting-wear characteristics of tubes, which are expressed in terms of the natural frequency and corresponding mode shape, are investigated.

2. Thermal Hydraulic Analysis

The basic parameters required for this fretting-wear prediction are the mass flux and tube-to-tube cross-flow gap velocity distributions of shell-side fluid flow, the effective mass (including both tube-side fluid mass and hydrodynamic mass) distribution of tube over the entire length of a specific U-tube under consideration, and the natural frequency and its corresponding mode shape of the tube.

The density and velocity distributions of shell-side flow field in a steam generator can be obtained from 3-dimensional two-phase thermal-hydraulic analysis. Several currently-used pressurized water reactor SG thermal-hydraulics codes are identified and among them ATHOS3 (Keeton and Singhal, 1986) is one of the most widely used codes for three-dimensional thermal-hydraulic analysis of steam generators, which is known to be a well documented and validated code. Thus, the ATHOS3 code is employed to calculate the secondary flow field of steam generator in this study.

The present calculation is performed for the steady-state conditions of the SGs at 100% power level because the potential tube damages such as fretting-wear and high-cycle fatigue during normal reactor operation has been addressed as one of the major safety issues of the operating reactors worldwide.

Due to the assumed planar symmetry about a vertical plane normal to the tube lane axis, in all ATHOS3 code calculations, only one half of the steam generator is considered for the calculations. The ATHOS3 models the flow region within the wrapper, above the tube sheet and below the steam separator entrance, and downcomer regions with finite difference mesh. The steam separators were accounted for by means of bulk models. The grid refinement in the U-bend region and the recirculated water entrance region, in the axial direction, was made for the purpose of obtaining the detailed flow conditions more precisely in such regions where the shell-side fluid is expected to flow with high cross-flow velocity.

The two-phase flows in steam generators can be simulated with the use of either homogenous model or algebraic slip model in the ATHOS3 calculations. While the homogenous model is defined on the basis of the assumption that the velocities of the liquid and vapor phases are equal in each of the three coordinate directions, in the algebraic slip model the liquid and vapor phases are assumed to move with unequal velocities in the vertical direction. As mentioned by Keeton and Singhal (1986), the algebraic slip model is considered to simulate more realistically than the homogeneous model since it accounts for slip between the two phases in the direction of predominant flow. Furthermore it was shown in reference (Singhal et al., 1991) that agreement of the calculation results with experimental data was always better when applying the algebraic slip rather than homogenous flow model. Thus, in this analysis, the algebraic slip model was employed. The magnitude of the velocity slip is calculated from empirical correlation, of which the default Lellouche-Zolotar option (Keeton and Singhal et al., 1986) was chosen for the present calculations.

Now, the normal-to-tube cross flow gap velocity over entire length of a specific U-tube is obtained from the ATHOS3 calculation results (Jo et al., 1992). The velocity components u_i, v_i and w_i in the circumferential, radial, and axial directions of the Cartesian coordinate at a point i on the specified tube can be calculated from the velocity components at 6 faces of the control cell including the point i by applying the interpolation method.

$$u_i = (1-\delta_x)u_W + \delta_x u_E \qquad (1a)$$

$$v_i = (1-\delta_y)v_S + \delta_y v_N \qquad (1b)$$

$$w_i = (1-\delta_z)w_B + \delta_z w_T \qquad (1c)$$

where δ_x, δ_y and δ_z are the distance-related interpolation coefficients and the subscripts E, W, N, S, T and B denote the east, west, north, south, top and bottom surfaces of the cell volume under calculation, respectively.

Considering the geometry of tube, the normal-to-tube cross-flow gap velocity $v_{n,g}$ can be expressed as

$$v_{n,g} = \left| v_i \cos\theta - u_i \sin\theta \right| \alpha_v \qquad \text{for the vertical straight tube section} \qquad (2)$$

$$v_{n,g} = \left| w_i \right| \alpha_h \qquad \text{for the horizontal straight tube section} \qquad (3)$$

$$v_{n,g} = \left| (v_i \cos\theta - u_i \sin\theta) \cos\varphi + w_i \sin\varphi \right| \alpha_v \qquad \text{for the U-bend tube section} \qquad (4)$$

where θ indicates the angle of the point i from the origin of polar coordinate on the horizontal cross-sectional plane containing the point i and φ is the angle of the point i on the half circle comprised of the U-bend arc and the chord connecting both end points of the arc. In addition, α_v is the coefficient for converting the velocity calculated with the ATHOS3 code using the continuum approach in conjunction with the porous media concept into the tube-to tube gap velocity, which is expressed as

$$\alpha_v = (1 - \beta_v) \frac{p}{p - d} \qquad (5)$$

where p and d indicate tube pitch and outer diameter of tube, respectively. And the blockage factor β_v varying with the type of tube array is expressed as

$$\beta_v = \frac{\pi}{4} \left(\frac{d}{p}\right)^2 \qquad \text{for the square tube array} \qquad (6)$$

$$\beta_v = \frac{\pi}{2\sqrt{3}} \left(\frac{d}{p}\right)^2 \quad \text{for the triangular tube array} \qquad (7)$$

Since the output of the ATHOS3 code calculation for density of the shell-side fluid is given as the representative values at the central points of control cells, the density distribution of shell-side fluid over the entire length of a specific U-tube under consideration also has to be determined from the 3-dimensional interpolations using the calculated density data at the central points of interfacial control cells and distance ratio factors.

One of the dynamic parameters for the present analysis is the distribution of effective (total) mass per unit length of the tube surrounded by the shell-side fluid. The effective mass per unit length of tube comprises the mass of tube, the mass of tube-side fluid, and the added mass resulting from the presence of shell-side fluid displaced by the tube (also called as hydrodynamic mass), which is expressed as

$$m_e(x) = m_t(x) + m_{pf}(x) + m_a(x) \qquad (8)$$

where m and x are mass per unit length of tube and the distance along the tube length from the upper surface of tube sheet, respectively. The subscripts of m in Eq. (8), e, t, pf and a denote effective, tube metal, primary fluid and added, respectively.

The added (hydrodynamic) mass m_a is defined as the equivalent mass of external fluid vibrating with the tube, which increases the effective mass of the tube in a fluid. The added mass of tube in a fluid is calculated by utilizing the semi-empirical correlation proposed by Pettigrew et al. (1994) based on the homogeneous two-phase density and on the equivalent diameter representing the confinement due to surrounding tubes.

3. Modal Analysis

Modal analyses using a commercial computer code ANSYS (2001) are performed to find the vibration characteristics of the U-tube. Four different types of U-tubes for SG Model 51 are chosen to investigate the wear characteristics as shown in Table 1 because they are located in the higher cross-flow velocities as compared to the interior of the tube bundle.

Full models are developed using the elastic straight pipe elements (PIPE16) for straight region and elastic curved pipe elements (PIPE18) for U-bend region. The U-tube consists of 62 PIPE16 elements in the straight region and 36 PIPE18 elements in the U-bend region as shown in Figure 1 for four different types of U-tubes.

The boundary conditions at the tube sheet nodes are fixed but the nodes at tube sheet plates and anti-vibration bars are free to move in the axial direction. The Block Lanczos method is used for the eigenvalue and eigenvector extractions to calculate 30 frequencies, which are composed of in-plane and out-of-plane modes.

The effective mass distribution along the entire tube was calculated from the thermal-hydraulic analysis. This mass density is used to find the vibration characteristics.

4. Wear-Rate Prediction

Connors (1981) investigated various ways of evaluating and correlating tube wear to tube motion and showed that the Archard's (1956) equation for adhesive wear can be applied to fretting wear as well as continuous sliding conditions.

$$V = K \cdot F_n \cdot L \qquad (9)$$

where V = volume of wear generated, K = wear coefficient (Figure 2), F_n = normal forces between surfaces and L = total sliding distance. While wear is not theoretically well defined and the Archard's equation is semi-empirical, it has been proved valuable in practical situations. Rubbing motion caused more wear than impacting motion, so Archard's equation can be used to evaluate tube wear due to foreign objects as well as between tube and tube support. Wear coefficients are shown in Figure 2 for various material combinations from some experimental data (Au-Yang, 2001).

An object in the moving fluid is subjected to the drag force, parallel to the relative approach velocity, and it exerts the normal force on the tube in the steam generator secondary side. The drag force can be calculated as

$$F_d = C_d \cdot A \cdot \rho \cdot \frac{v^2}{2g} \qquad (10)$$

where F_d = drag force, C_d = drag coefficient, A = area projected on to a plane normal to the direction of the velocity, ρ = density, v = fluid velocity and g = gravitational constant. The drag coefficient is dependent on the Reynolds number (Figure 3). It is difficult to predict what the Reynolds number will be because the structure in the secondary side of the steam generator is very complex, and therefore as a conservative estimate the maximum drag coefficients of Reynolds number $> 10^3$ are used.

The sliding distance can be calculated with the tube vibration amplitude due to the flow-induced vibration and the tube frequency. The sliding distance per cycle is four times the product of the tube vibration amplitude and the tube frequency and is calculated with

$$D = 4 \cdot C^* \sqrt{\left(\sum_{m=1}^{n} f_m \cdot d_{m,x} \cdot PF_{m,x} \right)^2 + \left(\sum_{m=1}^{n} f_m \cdot d_{m,z} \cdot PF_{m,z} \right)^2} \qquad (11)$$

where D = sliding distance per second, f_m = mth modal natural frequency of the steam generator tube, $d_{m,x}$ = modal displacement of mode m in x-direction, $d_{m,z}$ = modal displacement of mode m in z-

direction, $PF_{m,x}$ = modal participation factor of mode m in x-direction and $PF_{m,z}$ = modal participation factor of mode m in z-direction. Also, $C*$ is the factor which relates the root mean square (RMS) deflection from test or analysis to the amplitude of the modal analysis for a steam generator tube as follows:

$$RMS = C*\sqrt{\left(\sum_{m=1}^{n}d_{m,x}\cdot PF_{m,x}\right)^2 + \left(\sum_{m=1}^{n}d_{m,z}\cdot PF_{m,z}\right)^2} \tag{12}$$

Therefore the total sliding distance L in time t is determined from Eqs. (11) and (12) as

$$L = 4t\cdot RMS\cdot\frac{1}{\psi} \tag{13}$$

where

$$\psi = \sqrt{\left(\sum_{m=1}^{n}d_{m,x}\cdot PF_{m,x}\right)^2 + \left(\sum_{m=1}^{n}d_{m,z}\cdot PF_{m,z}\right)^2} \Bigg/ \sqrt{\left(\sum_{m=1}^{n}f_m\cdot d_{m,x}\cdot PF_{m,x}\right)^2 + \left(\sum_{m=1}^{n}f_m\cdot d_{m,z}\cdot PF_{m,z}\right)^2} \tag{14}$$

The wear volume generated on the tube is calculated using Eqs. (9), (10) and (13) as

$$V = 2Kt\cdot RMS\cdot C_d A\rho\frac{v^2}{g}\frac{1}{\psi} \tag{15}$$

The tube depth associated with this wear volume can be determined by defining the geometry of the wear scar. The geometrical relationship between wear volume and wear depth for a SG tube in contact with a flat bar is shown in Figure 4. Assuming that the tube and flat bar are perfectly aligned, the wear scar volume, V_s, is simply the area of interaction of a straight line and a circle of radius, R, multiplied by the flat bar width, l

$$V_s = \frac{R^2 l}{2}\left[2\alpha - \sin(2\alpha)\right] \tag{16}$$

where α is the contact angle (rad) and there are relations between the tube radius R, the wear depth h and scar width w as

$$\alpha = \cos^{-1}\left(1 - \frac{h}{R}\right) \tag{17}$$

$$w = 2R\cdot\sin\alpha \tag{18}$$

Equating the wear volume generated to the geometrically defined wear volume, the relationship between wear depth and time can be defined. Assuming a circular whirling pattern and neglecting the slope of the tube, area projected on to a plane normal to the direction of the fluid flow is

$$A = w\cdot l = 2Rl\cdot\sin\alpha \tag{19}$$

Therefore, the time required to wear into a tube to the minimum acceptable wall thickness h, which is usually defined as 40% through wall, is calculated from Eqs. (15) and (16)

$$t = \frac{gR\psi}{8KC_d\rho v^2\cdot RMS}\frac{2\alpha - \sin 2\alpha}{\sin\alpha} \tag{20}$$

Eq. (20) was derived based on the assumptions that the foreign object will remain in the same location once the tube wear begins and that only the tubes will experience wear. This can be used to calculate

the time required to wear completely through the tube wall. It should be noted that the tube could fail in fatigue before complete wear-through occurred.

5. Results and Discussion

Modal analyses are performed for four different types of U-tubes located in the higher cross-flow velocities as compared to the interior of the tube bundle and their frequencies and mode shapes are investigated for the fretting characteristics.

To investigate the effect of the internal pressure on the vibration characteristics of the tube, pressures are input as surface loads on the element surfaces of Type D. The resulting normalized frequencies with respect to the un-pressurized pipe are shown in Figure 5, which indicates that frequency changes are negligible up to the internal pressure of about 10 MPa. Above this pressure, frequency drops very rapidly with the increase of the pressure. The normalized frequencies can be represented for all modes as

$$\lambda = 148522 \cdot \exp\frac{-P}{3.9217E13} - 148521 \tag{21}$$

where λ and P are the normalized frequency and the internal pressure (Pa), respectively. When considering that pressure difference during normal operation of the nuclear power plant is almost 5 MPa, frequency difference can be concluded to be negligible with the inclusion of the internal pressure.

ψ defined in Eq. (14) is calculated for four different types of tube from modal analyses results at node 6 where the foreign object is assumed to rest on and is summarized in Table 2. Because the time required to wear is proportional to ψ, their remaining lives are almost the same for the same flow velocity. If only fundamental natural frequency is considered in calculating ψ, the remaining life of the tube is over estimated as shown in Table 2 by about 2 times. Therefore, care should be taken for the remaining life of the tube not to be over estimated by including the sufficient number of modes in the calculation of ψ. Figure 6 shows cumulative mass fraction and ψ with respect to the total number of modes under consideration, which shows that in calculating ψ more than 80% of the cumulative mass fraction should be considered not to overestimate the remaining life of the tube.

The effect of internal pressure on the remaining life of the tube may be investigated by calculating ψ for modal analyses results with the inclusion of the internal pressure. ψ for Type D is summarized in Table 3 and Figure 7, which indicates that the effect of internal pressure on the remaining life of the tube due to foreign object is negligible with the inclusion of the internal pressure during normal operation of the nuclear power plant. This can be predictable from the fact that frequency changes are negligible up to the internal pressure of about 10 MPa.

The effect of flow velocity on the remaining life of the tube may be investigated from Eq. (14) where time required to wear is inversely proportional to the square of the flow velocity and is shown in Figure 8. Therefore it is noted that the flow velocity is the most significant factor to determine the remaining life of the tube.

6. Conclusions

Derived in this paper is the formula to predict the remaining life of the U-tube which is subject to fretting wear by a foreign object. The time required to wear the tube is calculated based on the Archard's equation and several parameters are investigated for the effect on the life of the U-tube, generating the following conclusions:

1) Sufficient number of modes should be considered to calculate the time required to wear the tube.

2) Frequency changes of the tube are negligible with the inclusion of the internal pressure during the normal operation and therefore fretting-wear characteristics are not affected by the internal pressure of the tube.

3) The remaining life of the tube depends on the flow velocity by inverse proportion of the square velocity and the flow velocity is the most significant factor to the time required to wear the tube.

References

1. Archard, J. F., and Hirst, T., 1956, The Wear of Metals under Unlubricated Conditions, *Proceedings of the Royal Society of London*, **A(236)**, p.397.
2. ANSYS, 2001, *ANSYS Structural Analysis Guide*, ANSYS, Inc., Houston.
3. Au-Yang, M. K., 2001, *Flow-induced Vibration of Power and Process Plant Components*, ASME Press, New York.
4. Chen, S. S., and Chung, H., 1976, *Design Guide for Calculating Hydrodynamic Mass, Part 1 : Circular Cylindrical Structures*, ANL-CT-76-45, Argonne National Laboratory, Argonne, IL.
5. Connors, H. J., 1981, Flow-Induced Vibration and Wear of Steam Generator Tubes, *Nuclear Technology*, **55**, pp.311-331.
6. Jo, J. C. et al., 1992, *A Study on the Thermal-hydraulic and Flow-induced Tube Vibration Analysis of Nuclear Steam Generators*, KINS/AR-198, Korea Institute of Nuclear Safety, Daejeon, Korea.
7. Keeton, L. W., and Singhal, A. K., 1986, *ATHOS3 : A Computer Program for Thermal Hydraulic Analysis of Steam Generators*, NP-4604-CCM, Electric Power Research Institute, Palo Alto, CA.
8. Lindeburg, M. R., 1994, *Mechanical Engineering Reference Manual*, 9th ed., Professional Publications, Inc.
9. Pettigrew, M. J., and Taylor, C. E., 1994, Two-Phase Flow-Induced Vibration: An Overview, *ASME Journal of Pressure Vessel Technology*, **116**, pp.233-253.
10. Pettigrew, M. J., Taylor, C. E., and Kim, B. S., 1989, Vibration of Tube Bundles in Two-Phase Cross-Flow : Part 1 – Hydrodynamic Mass and Damping, *ASME Journal of Pressure Vessel Technology*, **111**, pp.466-477.
11. Singhal, A. K., and Srikantiah, G. S., 1991, A Review of Thermal Hydraulic Analysis Methodology for PWR Steam Generators and ATHOS3 Code Applications, *Progress in Nuclear Energy*, **25(1)**, pp.7-70.

Table 1. Geometric description of tube bundle

Parameters	Type A	Type B	Type C	Type D
Outer diameter (10^{-2} m)	2.2225	2.2225	2.2225	2.2225
Inner diameter (10^{-2} m)	1.968	1.968	1.968	1.968
Tube thickness (10^{-3} m)	1.27	1.27	1.27	1.27
Radius of curvature of U-bend region (m)	0.3458	0.3810	0.8041	1.5200
Number of tube support plates	7	7	7	7
Number of AVB support points in U-bend region	0	1	2	4
Angle of curved spans (^{o})	0	90	50, 80	35, 40

Table 2. ψ for tube bundles

Tube type	Mode numbers considered		
	1 ~ 30	1 ~ 20	1
A	0.0155	0.0156	0.0439
B	0.0156	0.0158	0.0307
C	0.0155	0.0153	0.0305
D	0.0158	0.0159	0.0310

Table 3. ψ for internal pressure variations of Type D

Pressure (Pa)	Mode numbers considered		
	1 ~ 30	1 ~ 20	1
0	0.0158	0.0159	0.0310
1.0E6	0.0158	0.0159	0.0311
1.0E7	0.0160	0.0160	0.0320
1.0E8	0.0176	0.0178	0.0504
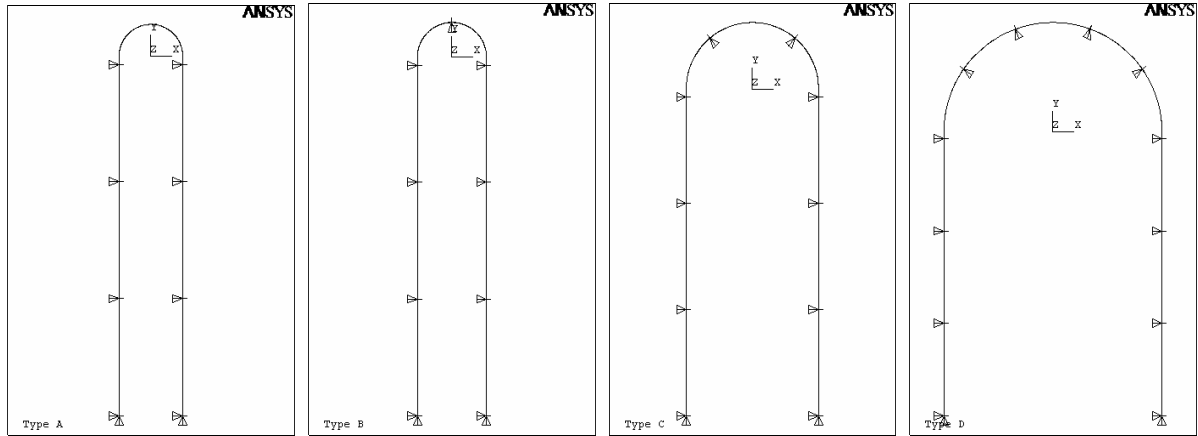
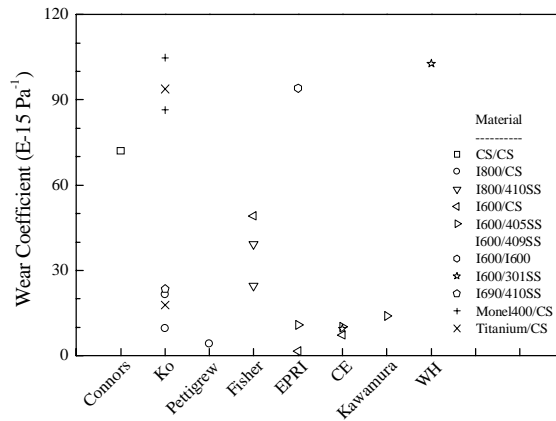Figure 1. Finite element models of U-tube

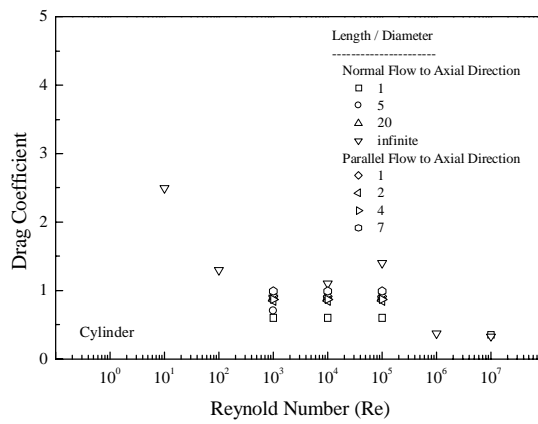Figure 2. Wear coefficients for various material combinations

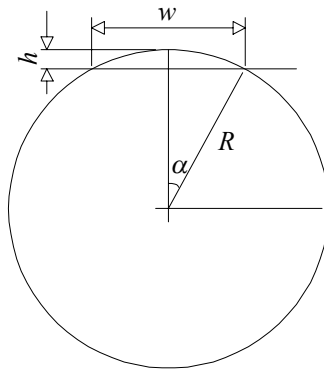Figure 3. Drag coefficients (Lindeburg, 1994)
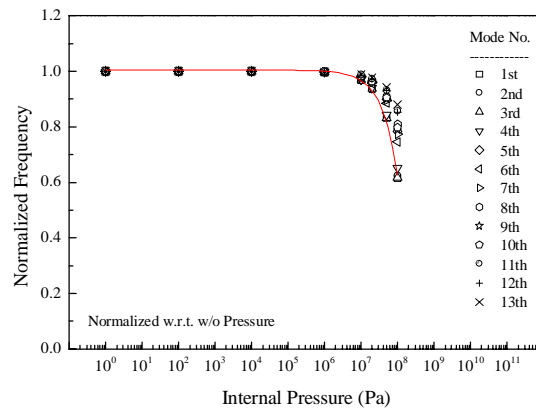
Figure 4. Contact between tube and flat bar

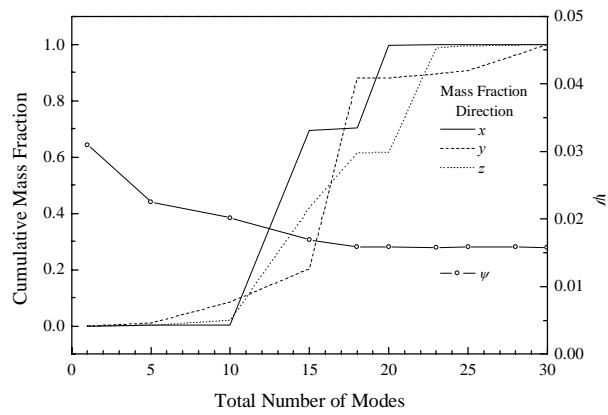Figure 5. Normalized frequency variations with respect to w/o internal pressure case

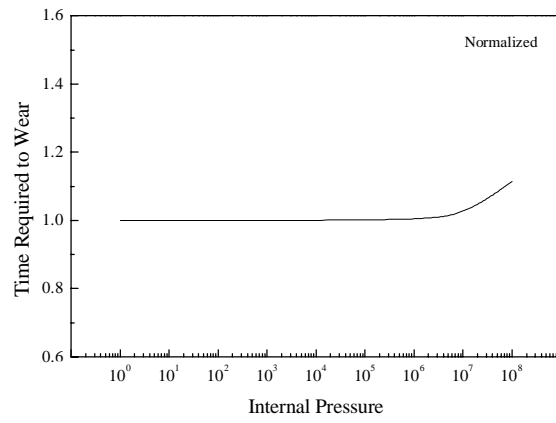Figure 6. Cumulative mass fraction and ψ vs. total number of modes
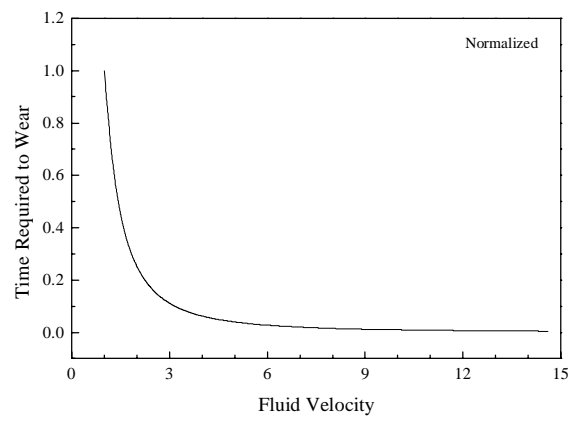
Figure 7. Time required to wear vs. internal pressure

Figure 8. Time required to wear vs. fluid velocity